RAPID COMMUNICATIONS

PHYSICAL REVIEW B VOLUME 49, NUMBER 1 1 JANUARY 1994-I

Particle-size effects on the value of T_c of $MnFe_2O_4$: Evidence for finite-size scaling

G. U. Kulkarni, K. R. Kannan, T. Arunarkavalli, and C. N. R. Rao*

Council for Scientific and Industrial Research Centre of Excellence in Chemistry and Solid State and Structural Chemistry Unit, Indian Institute of Science, Bangalore 560 012, India

(Received 10 August 1993)

^{57}Fe Mössbauer measurements show that the T_c of $\langle 12 \rangle$-nm particles of $MnFe_2O_4$ is higher than that of the $\langle 33 \rangle$-nm particles, which exhibit the bulk T_c value (573 K). The ^{57}Fe isomer shift as well as the internal field are, however, independent of the particle size, as is the cation distribution determined by Mn and Fe extended x-ray absorption fine structure and Mn x-ray absorption near-edge structure measurements at different temperatures. The results confirm that the higher T_c of the $\langle 12 \rangle$-nm particles arises from finite-size scaling.

Size-dependent properties of nanoscale particles have attracted considerable attention in recent years.[1–4] Of particular interest is the question of what happens to magnetic properties when the particle size is of the order of a domain. Experimental studies of small magnetic particles have by and large been limited to superparamagnetism in very small particles.[5,6] Tang *et al.*[1] have recently measured the Curie temperature of ferrimagnetic $MnFe_2O_4$ particles and found a significant increase in T_c (relative to the bulk value) in particles slightly larger than the superparamagnetic critical size. The authors explain this interesting observation on the basis of the finite-size scaling model,[7] according to which the relative enhancement in T_c is related to the particle diameter raised to an exponent. This explanation has been questioned by some workers[8,9] who consider that particle-size-dependent changes in the cation distribution over tetrahedral and octahedral sites could as well be responsible for the increase in T_c. Considering the importance of the problem,[10] we have reexamined the properties of $MnFe_2O_4$ particles employing atom-specific probes. We have probed the magnetic environment around the Fe ions by ^{57}Fe Mössbauer spectroscopy, as particles of different sizes undergo the ferrimagnetic-paramagnetic transition. We have monitored the local environment of the Mn and Fe ions as a function of size as well as temperature by means of the Mn K and Fe K extended x-ray absorption fine structure (EXAFS). In addition, we have examined the Mn x-ray absorption near-edge structure (XANES) in order to study the distribution of Mn in the different valence states. The present study has shown that the cation distribution remains essentially the same in $MnFe_2O_4$ particles of different sizes and that there is indeed a ferrimagnetic phase comprising of small ferrite particles ($\sim$12 nm) with a T_c higher than that of the bulk spinel.

$MnFe_2O_4$ particles of varying sizes (6–33 nm) were prepared following the procedure in the literature.[11] The samples were annealed in helium at 773 K for 1 h and slowly cooled to room temperature in order to ensure equilibrium cation distribution. The cation stoichiometry was checked by energy dispersive analysis of x rays and the single crystal nature of the particles was verified by high-resolution electron microscopy. Mean sizes of the particles was obtained from the Brunauer-Emmett-Teller surface areas. Samples with mean particle diameters of 9, 12, and 33 nm were chosen for detailed studies. Mössbauer and EXAFS measurements were carried out by taking the samples in the form of wafers. For the EXAFS measurements, a Ge(220) crystal was used as the monochromator on a Rigaku spectrometer attached to a rotating anode x-ray source (RU 200B, Rigaku, Japan). Fourier transforms (FTs) of the EXAFS data were obtained with $k_{min} \sim 3$ and $k_{max} \sim 12$ Å^{-1} after weighing the data by k^3.

^{57}Fe Mössbauer spectra show the sextet due to the ferrimagnetic species or/and a doublet due to the para and/or superparamagnetic species, depending on the size and temperature (Fig. 1). The 300-K spectrum of the $\langle 33 \rangle$-nm particles show a six finger pattern indicating that all iron ions are in the magnetic phase. The internal magnetic field (H_{int}) was found to be 463 KOe when the spectrum was fitted with a single sextet. The spectrum could also be fitted with two sextets (75:25) with H_{int} values of 456 and 484 kOe corresponding to two Fe sites in the spinel lattice, but with nearly the same isomer shift (IS $\sim$0.4 mm s^{-1}). At 573 K (T_c of bulk $MnFe_2O_4$), the $\langle 33 \rangle$-nm particles show a doublet in the Mössbauer spectrum along with a broad singlet. The $\langle 9 \rangle$-nm particles exhibit Mössbauer spectra characteristic of small superparamagnetic particles (Fig. 1), showing the ferrimagnetic sextet a very low temperatures (H_{int} 490 kOe at 90 K). While there can be no sharp T_c for such a sample, ferrimagnetism does not manifest itself down to $\sim$200 K. However, the isomer shift in the $\langle 9 \rangle$-nm sample is the same ($\sim$0.4 mm s^{-1}) as that of the $\langle 33 \rangle$-nm particles.

The behavior of the $\langle 12 \rangle$-nm sample is interesting in that the Mössbauer spectrum which is composed of a sextet (ferrimagnetic) and a doublet (superparamagnetic) at 300 K continues to show the sextet even at 573 K (Fig. 1). The sextet disappears only above 620 K, clearly indicating that the T_c of the $\langle 12 \rangle$-nm particles is higher than that of the $\langle 33 \rangle$-nm particles by $\sim$50 K. We present the results of the Mössbauer studies in terms of the variation of the ferrimagnetic fraction at 573 K as well as of T_c

 ©1994 The American Physical Society

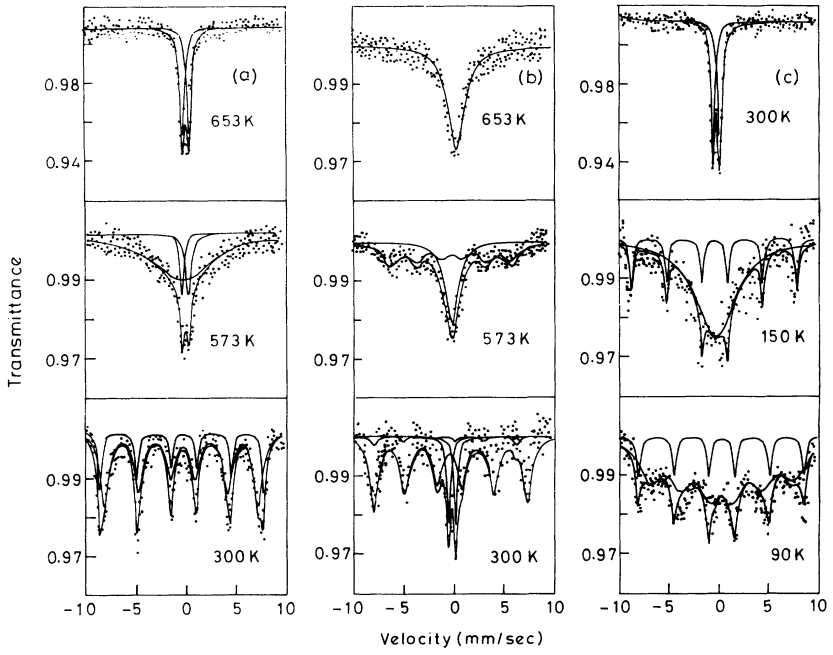

FIG. 1. ^{57}Fe Mössbauer spectra of the ferrite samples at various temperatures. Particles with means diameters of (a) 33 nm, (b) 12 nm, and (c) 9 nm.

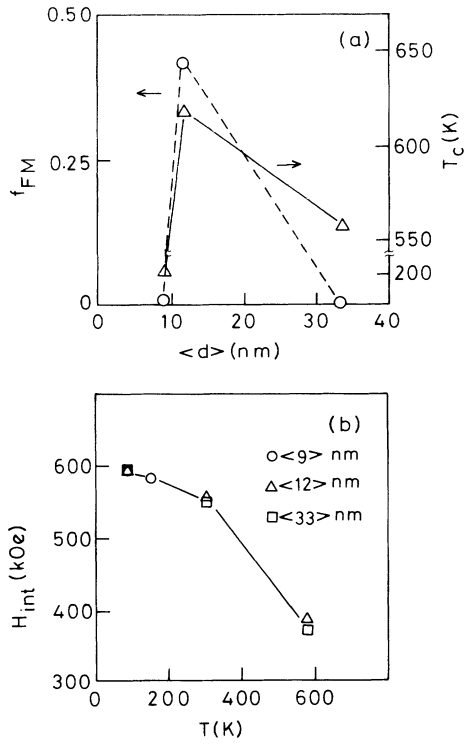

FIG. 2. (a) Variation of the fraction of ferrimagnetic particles (circles) at 573 K (bulk T_c value) and T_c of $MnFe_2O_4$ (triangles) with particle size. In case of the ⟨9⟩-nm particles, we have shown T_c as the temperature at which ferrimagnetism first manifests itself in the Mössbauer spectrum. (b) Variation of the internal magnetic field, H_{int} with temperature for the ⟨33⟩-, ⟨12⟩-, and ⟨9⟩-nm particles.

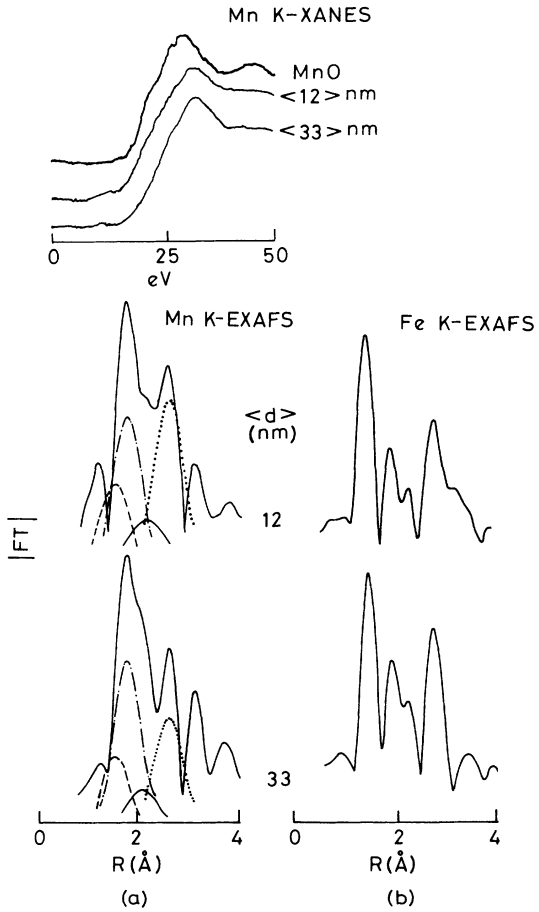

FIG. 3. Fourier transforms (FTs) of the EXAFS of the ferrite samples at room temperature: (a) Mn K EXAFS and (b) Fe K EXAFS. Fourier deconvoluted peaks corresponding to different oxygen coordinations are also shown. The peak due to metal-metal coordination is shown by the dotted line. The inset in (a) shows Mn K near-edge spectra of the ferrite samples along with that of MnO.

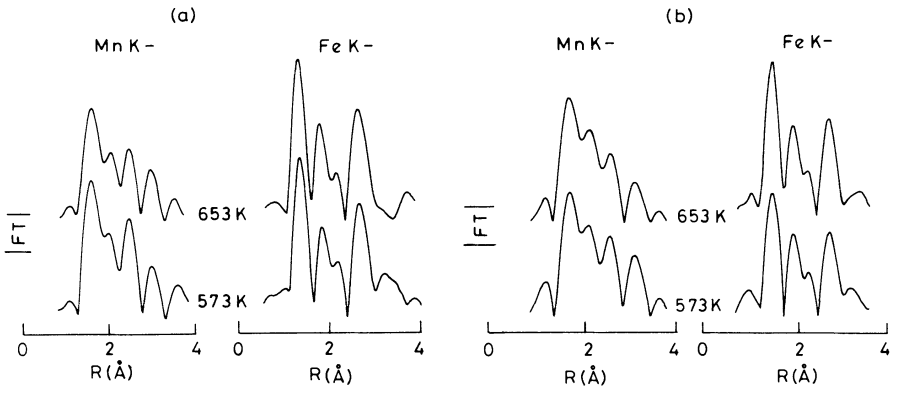

FIG. 4. Fourier transforms of Mn K and Fe K EXAFS of the ferrite samples at 573 and 653 K. (a) The ⟨33⟩-nm particles and (b) the ⟨12⟩-nm particles.

with the particle size. We show in Fig. 2(b) how the H_{int} remains essentially the same in samples of different particle sizes (~490–495 kOe at 90 K). The near constancy of the isomer shift and H_{int} in samples of different particle sizes indicates that the cation distribution does not change with particle size. It, therefore, appears that the higher T_c of the ⟨12⟩-nm sample is due to finite-size scaling. By employing the finite-size scaling formula we estimate the T_c of the ⟨12⟩-nm particles to be 617 K, which agrees with the experimental value (620 K) found by us. The correlation length exponent is 1.42 and the amplitude is 2 nm.

In order to ensure that the increase in T_c of the ⟨12⟩-nm sample relative to the ⟨33⟩-nm sample is not due to changes in cation distribution and related factors, we have examined the local environment of Fe and Mn ions by EXAFS. The FT of the Mn K EXAFS of the ⟨33⟩-nm sample at 300 K (Fig. 3) shows the main feature at 1.8 Å with a shoulder around 2.1 Å due to oxygen coordination. By appropriate analysis of the data by the residual FT method[12] (r window: 1.4–2.9 Å) by employing MnO parameters, we obtain Mn-O distances of 2.0, 2.22, and 2.52 Å with coordinations of 2.0, 4.5, and 1.2. The 2.22-Å distance is due to the tetrahedral site, the other two distances arising from the John-Teller distorted octahedra. The proportion of octahedral Mn is estimated to be ~32% consistent with the degree of inversion reported in the literature.[13] The FT of the ⟨12⟩-nm sample (Fig. 3) gave Mn-O distances and coordination close to those of the ⟨33⟩-nm sample. Mn K XANES is similar in ferrite samples of different sizes (see inset of Fig. 3) indicating identical average oxidation states of Mn (estimated to be 2.32) and hence the degree of inversion. FTs of the Mn K EXAFS of the ⟨33⟩ and ⟨12⟩ nm were nearly identical at at 573 and 653 K (Fig. 4). The first main feature in the FTs at these temperatures was at a lower distance since the proportion of octahedral Mn was higher (~60%) than at 300 K.

Fourier transforms of the Fe K EXAFS of the ⟨33⟩-nm sample at 300 K show distinct features due to oxygen coordination at 1.85, 2.24, and 2.70 Å (Fig. 3) which on curve-fitting analysis gave Fe-O distances of 1.88, 2.33, and 2.73 Å. The 2.33-Å distance is ascribed to the tetrahedral site and the other two to the octahedral site. The ratio of octahedral to tetrahedral Fe sites was 0.57. This ratio as well as the Fe-O distances are found to be the same in the ⟨12⟩-nm sample. The FTs at 573 and 653 K were also nearly identical for the ⟨12⟩- and ⟨33⟩-nm samples (Fig. 4) but the proportion of the tetrahedral species was higher than at 300 K.

The present EXAFS study establishes that the cation distribution and the associated features remain essentially the same in the ⟨12⟩- and ⟨33⟩-nm samples (Table I), thus reinforcing the suggestion that the higher T_c of the ⟨12⟩-nm sample is likely to be due to finite-size scaling.

TABLE I. Structural parameters of $MnFe_2O_4$ particles.

	Coordination number and distances for Mn-O				Coordination numbers and distances for Fe-O			
	⟨12⟩-nm particles		⟨33⟩-nm particles		⟨12⟩-nm particles		⟨33⟩-nm particles	
T (K)	N	R (Å)	N	R (Å)	N	R (Å)	N	R (Å)
300	4	1.97	4	2.00	4	1.90	4	1.88
	4	2.20	4	2.22	4	2.32	4	2.33
	2	2.54	2	2.52	2	2.74	2	2.74
573	3	2.05	3	2.05	3	1.89	4	1.90
	2	2.20	2	2.20	3	2.33	4	2.35
	3	2.53	3	2.53	3	2.74	2	2.75
653	3	2.06	4	2.06	4	1.89	4	1.89
	3	2.19	2	2.20	3	2.34	3	2.33
	3	2.50	2	2.50	2	2.73	2	2.75

*Author to whom correspondence should be addressed.

[1]Z. X. Tang, C. M. Sorensen, K. J. Klabunde, and G. C. Hadjipanayis, Phys. Rev. Lett. **67**, 3602 (1991).

[2]T. Sato, T. Iijima, M. Seki, and N. Inagaki, J. Magn. Magn. Mater. **65**, 252 (1987).

[3]R. P. Andres, R. S. Overback, W. L. Brown, L. E. Brus, W. A. Goddard III, A. Kaldor, S. G. Louie, M. Moscovitis, P. S. Peercy, S. J. Riley, R. W. Seigle, F. Spaepen, and Y. Wang, J. Mater. Res. **4**, 704 (1989).

[4]S. Gangopadhyaya, G. C. Hadjipanayis, B. Dale, C. M. Sorensen, K. J. Klabunde, V. Papaefthymiou, and A. Kostikas, Phys. Rev. B **45**, 9778 (1992).

[5]T. Shinjo, T. Shigematsu, N. Hosaito, T. Iwasaki, and T. Takai, J. Appl. Phys. **21**, L220 (1982).

[6]W. Kundig, H. Bommel, G. Constabaris, and R. H. Lindquist, Phys. Rev. B **142**, 327 (1966).

[7]M. N. Barber, in *Phase Transitions and Critical Phenomena,* edited by C. Domb and J. L. Lebowitz (Academic, New York, 1983), Vol. 8, p. 145.

[8]P. J. van der Zaag, A. Noordermeer, M. T. Johnson, and P. F. Bongers, Phys. Rev. Lett. **68**, 3112 (1992).

[9]V. A. M. Brabers, Phy. Rev. Lett. **68**, 3113 (1992).

[10]Z. X. Tang, C. M. Sorensen, K. J. Klabunde, and G. C. Hadjipanayis, Phys. Rev. Lett. **68**, 3114 (1992).

[11]Z. X. Tang, C. M. Sorensen, K. J. Klabunde, and G. C. Hadjipanayis, J. Colloid Interface Sci. **146**, 38 (1991).

[12]G. U. Kulkarni, G. Sankar, and C. N. R. Rao, Z. Phys. B **73**, 529 (1989).

[13]M. A. Denecke, W. Gunsser, G. Buxbiun, and P. Kuske, Mater. Res. Bull. **27**, 507 (1992).